Maintained memory and long-term potentiation in a mouse model of Alzheimer's disease with both amyloid pathology and human tau

EJN Journal Section: Clinical and Translational Neuroscience

Maintained memory and long-term potentiation in a mouse model of Alzheimer's disease with both amyloid pathology and human tau

Jane Tulloch[1], Olga Netsyk[1], Eleanor K Pickett[1], Abigail G Herrmann[1], Pooja Jain[1], Anna J Stevenson[1], Iris Oren[1], Oliver Hardt[2,3]*, and Tara L. Spires-Jones[1]*

1. The University of Edinburgh Centre for Discovery Brain Sciences and UK Dementia Research Institute, 1 George Square, Edinburgh, EH8 9JZ UK
2. McGill University, Department of Psychology, Montreal QC H3A 1B1, Canada
3. The Simons Initiative for the Developing Brain and The Patrick Wild Centre, The University of Edinburgh, Edinburgh, United Kingdom

*Equal contributions and co-corresponding authors

Contact:
Tara L. Spires-Jones, D. Phil The University of Edinburgh Centre for Discovery Brain Sciences and UK Dementia Research Institute 1 George Square Edinburgh EH8 9JZ UK Phone: +44(0) 131 651 1895 Fax: +44(0) 131 651 1832 Tara.Spires-Jones@ed.ac.uk
Oliver Hardt - oliver.hardt@mcgill.ca

Running title: Maintained memory and plasticity in a model of Alzheimer's
Pages: 20
Figures: 3
Tables: 1
Words in manuscript: 7713
Words in abstract: 162

Keywords: LTP, dementia, novel object recognition, behaviour

Abbreviation List:

AD – Alzheimer's disease

APP – amyloid precursor protein

Aβ – amyloid beta

PS1 – presenilin 1

LTP – long-term potentiation

NA – numerical aperture

NMDG - N-methyl-D-glucamine

Ser - serine

Abstract:

One of the key knowledge gaps in the field of Alzheimer's disease research is the lack of understanding of how amyloid beta and tau cooperate to cause neurodegeneration. We recently generated a mouse model (APP/PS1+Tau) that develops amyloid plaque pathology and expresses human tau in the absence of endogenous murine tau. These mice exhibit an age-related behavioural hyperactivity phenotype and transcriptional deficits which are ameliorated by tau transgene suppression. We hypothesized that these mice would also display memory and hippocampal synaptic plasticity deficits as has been reported for many plaque bearing mouse models which express endogenous mouse tau. We observed that our APP/PS1+Tau model does not exhibit novel object memory or robust long-term potentiation deficits with age, whereas the parent APP/PS1 line with mouse tau did develop the expected deficits. These data are important as they highlight potential functional differences between mouse and human tau and the need to use multiple models to fully understand Alzheimer's disease pathogenesis and develop effective therapeutic strategies.

Introduction:

Alzheimer's disease (AD) is neuropathologically defined by brain atrophy and the accumulation of amyloid plaques and neurofibrillary tangles. Amyloid pathology develops very early in the disease process, and rare disease-causing mutations all act through impacting amyloid beta (Aβ) accumulation; however, tau accumulation in neurofibrillary tangles is more closely associated with neurodegeneration and dementia symptoms. These data led to the theory that Aβ initiates the disease

process causing downstream changes in tau that lead to neurodegeneration (Hardy & Higgins, 1992).

Soluble forms of Aβ cause synaptic dysfunction and loss with deficits in long-term potentiation (LTP) and plaque-associated synapse degeneration observed robustly across many model systems (Koffie *et al.*, 2009, 2011; Li *et al.*, 2009; Klein, 2013; Spires-Jones & Hyman, 2014). Further, many mouse models that develop amyloid pathology due to expression of familal AD genes and those that express both amyloid and human mutant tau associated with human tauopathies develop spatial memory deficits as assessed by behavioural tests including the water maze and novel object recognition (Oddo *et al.*, 2003; DaRocha-Souto *et al.*, 2011; Masuda *et al.*, 2016; Sasaguri *et al.*, 2017). An OVID-Medline search for papers pubished between 1946 and June 2020 generated 56 results (search terms with the terms (Amyloid beta-Peptides OR Amyloid) AND (tau Proteins OR Tauopathies) AND Mice AND (Memory OR Long term potentiation)). Of these, the vast majority (43) were studies looking at interventions that changed memory or LTP in mouse models of AD, without examining the interplay of Aβ and tau. Only 3 of these papers specifically studied the interactions of these two pathological proteins in memory or LTP. First, in mice expressing APP with the arctic mutation and wild-type human tau, genetic reduction of β-site APP cleaving enzyme (BACE) which lowered soluble Aβ levels improved memory concomitant with a reduction in mislocalisation of tau to post synapses (Chabrier *et al.*, 2012). Secondly, brain slices from tau knockout mice do not exhibit LTP inhibition upon application of exogenous soluble Aβ, indicating

interplay between Aβ and tau in LTP phenotypes (Shipton *et al.*, 2011). Third, in mice with amyloid pathology, tau knockout prevented spatial memory deficits (Roberson *et al.*, 2007). Several more studies suggest that lowering endogenous mouse tau levels protects against other synaptic phenotypes in mice with plaques (Ittner *et al.*, 2010; Vossel *et al.*, 2010; Roberson *et al.*, 2011; DeVos *et al.*, 2018). However, many of these studies looking at interplay between Aβ and tau in memory and synaptic plasticity are complicated by the presence of endogenous mouse tau, which is different from human tau and thus may have different functional properties. Recent data also indicate that the interplay between Aβ and tau is more complex than a linear cascade and likely involves glia and neuron-glia interactions (Henstridge *et al.*, 2019).

We recently developed a mouse model without endogenous mouse tau (MAPTnull) which expresses human familial AD mutant amyloid precursor protein (APP) and presenilin 1 (PS1) and reversibly expresses human tau (APP/PS1+Tau mice) (Pickett *et al.*, 2019). These mice develop plaques, increases in inflammatory gene expression, and decreses in synaptic gene expression, and an age-related hyperactivity phenotype (Pickett *et al.*, 2019). In this study, we tested the hypothesis that these APP/PS1+Tau mice would exhibit synaptic plasticity and memory deficits at the age when we previously observed behavioural and transcriptional phenotypes. To do this, APP/PS1+Tau mice and APP/PS1 mice with endogenous mouse tau were tested for novel object recognition memory and LTP.

Methods:

Subjects

APP/PS1+Tau mice were bred as previously described (Pickett *et al.*, 2019). Briefly, all mice in this colony had no endogenous mouse tau (homozygous MAPTnull, FVB.*Mapt*$^{tm1(EGFP)Klt}$ (Tucker *et al.*, 2001)), and feeder lines expressed (1) human Swedish mutant amyloid precursor protein and presenilin 1 delta exon 9 under control of the Thy1 promoter (B6C3-Tg(APPsw,PSEN1dE9)85DboMm, (Jankowsky *et al.*, 2004)) and a tetracycline transactivator transgene downstream of a calcium calmodulin kinase II promotor (CKtTA, B6.Cg-(Camk2a-tTA)1/MmayDboJ (Yasuda & Mayford, 2006)) and (2) human 0N4R tau under the control of a dox-off tetracycline transactivator promotor (FVB-Tg(tetO-0N4R-MAPTwt)21221, (Hoover *et al.*, 2010)). The two feeder lines were crossed to generate 4 experimental genotypes all MAPTnull: control mice expressing neither transgene, mice expressing the APP/PS1 transgene only (APP/PS1), mice expressing the tau transgene only (Tau), and mice expressing both the APP/PS1 and tau transgenes (APP/PS1+Tau). One cohort of APP/PS1+Tau mice was tested for novel object recognition and open field behaviour at 3, 6, and 9 months of age with rotarod testing at 9 months. This cohort was sacrificed at 9 months of age and some brains used for the LTP study. Another

cohort of littermates was tested for novel object recognition memory, open field behaviour, and rotarod at 10.5 and 14.5 months of age to ensure we had not tested mice too young to observe a memory phenotype. APP/PS1 and CKtTA mice with endogenous mouse tau and their littermate controls were also tested at 9-10 months of age. Supplemental tables 1-4 contain data from each mouse tested in these experiments. Table 1 shows a summary of the mice used in this paper.

Animal work was carried out in accordance with the Animals [Scientific Procedures Act] 1986 (UK) and the council directive 2010/63EU of the European Parliament and the Council of 22 September 2010 on the protection of animals used for scientific purposes.

Novel object recognition and open field testing

Animals were tested for novel object recognition in a square box (40 x 40 x 60 cm) made of dark opaque walls (laminated MDF) with approximately 2.5 cm of corn cob bedding on the floor of the arena. Animals were recorded using an overhead camera and the video signal was fed into Blackmagic Media Express computer software which captured the movement of the animals. Each day animals were brought into the testing room in their home cage upon the end of the 12 h dark cycle and allowed to settle for 1 hour. Individual experiments were composed of 3 phases: habituation, sampling and probe, with all experiments performed in the morning. For habituation, animals were

exposed to the open field in the absence of any objects for 4 consecutive days. On day 1, animals were introduced to the centre of the arena along with cage mates for 20 min. For days 2-4, individual animals were exposed to the arena for 10 min per day, being placed into the open field facing a different corner of the arena each day, the sequence of which was assigned using a random number generator. For each experimental group, the order in which animals were placed in the arena was randomly assigned using a random number generator. On day 4 of habituation, open field exploration was recorded for 10 minutes using an overhead camera. These data were published previously (Pickett *et al.*, 2019); here the 9-10.5 month old data are shown in figure 1a for reference purposes.

Following habituation, individual mice participated in a sampling phase of 3 sampling trials and 1 probe trial. For the sampling phase (which took a total of 30 minutes per mouse), animals were exposed 3 times to 2 identical objects for 5 min followed by 5 min in a holding cage (35 x 15 x 15 cm) that was identical to their home cages. The objects remained in the same location during sampling, in two opposing corners of the open field, each object put 10 cm from the corner. After the sampling phase animals were returned to their home cage. The bedding on the floor of the arena was mixed through to disperse odors, any waste material was removed, and objects were cleaned with alcohol between mice. Probe trials were conducted 24 h after sampling and consisted of a single 3 min exposure to 2 objects (1 familiar object from the sampling phase and 1 novel object, both objects placed at the locations objects occupied during

sampling), followed by 5 min in the holding cage prior to return to the home cage. Once all trials were completed each day, mice remained in the testing room for 1 h to rest prior to return to the holding room.

Over the course of an experiment each mouse participated three times in this task, with 1 day between iterations. Each time, different objects were used. In each probe trial we paired two objects that elicited comparable exploratory activity as determined in a previous study in naïve mice. This way we ensured that pre-existing object preferences did not bias behavior in the probe trials. The objects used in sampling and probe phases were counterbalanced across genotypes and repetitions of this task to ensure comparison between groups. Exploration was determined in a blind manner using in-house software (available upon reasonable request from corresponding author O.H.). Individual probe trials were manually scored, with exploration defined as a mouse being within 2 cm of an object, directing its nose at the object and being involved in active exploration such as sniffing or whisking. For each probe phase, a discrimination index (d) was calculated ((time exploring novel object – time exploring familiar object)/(time exploring both objects)). Mice are attracted to novelty, and values of $d > 0$, indicating that they prefer exploring the novel object, suggest that they have memory for the object encountered during sampling. Values of $d = 0$ indicate mice treat both objects the same, and this absence of novelty preference suggests that they no longer express memory for the object encountered during sampling. Probe trials in which a mouse did not reach at least 10 s of total exploratory activity of objects were

excluded from the analysis. Effect size was calculated for wild-type mice with n=6 showing a mean of 0.296, standard deviation of 0.145 and Cohen's d effect size of 2.041, indicating that groups of at least 6 have more than sufficient power to detect intact novel object recognition memory. Group sizes for our experiments are outlined in Table 1.

Rotarod testing

To test motor function, mice were tested with a Rotarod (IITC Life Science) for 4 consecutive days. Each day animals were brought into the testing room in their home cage and allowed to settle for 1 h. Animals were placed on the Rotarod in separate lanes with male and female mice running in separate trials. Each day, mice participated in 3 baseline trials and 7 training trials, no trial lasting longer than 90 s. Baseline trials consisted of 3 trials separated by 2-min long rests between trials. During baseline trials, the drums rotated at a constant speed of 4 rotations per minute. Thirty minutes after the baseline trials, mice underwent 7 experimental trials with 2-min long rests in between. During the training trials, the rotational speed of the drums accelerated, from a starting speed of 4 rotations per minute to a final speed of 25 rotations per minute that was reached within 60 s. The average latency to fall off of the rotarod in experimental trials on the last day of testing was used to compare groups of genotypes. Data from mice who consistently jumped off of the rotarod (as opposed to running until they fell) were excluded from the analysis.

Electrophysiology

Electrophysiology experiments were performed with the experimenter blind to genotype. Acute horizontal brain slices were prepared as follows. Mice were deeply anaesthetized by the inhalation of isoflurane followed by intra-peritoneal injection of pentobarbital (20%, 0.7□l/g). Animals were transcardially perfused with oxygenated (95% O_2, 5% CO_2) protective NMDG-based solution of the following content (mM): 92 N-methyl-D-glucamine (NMDG), 2.5 KCl, 1.25 NaH_2PO_4, 30 $NaHCO_3$, 20 HEPES, 25 glucose, 5 Na-ascorbate, 3 Na-pyruvate, 0.5 $CaCl_2$, and 10 $MgCl_2$, pH 7.3–7.4 (titrated with 5M HCl). The mouse was decapitated and the brain was quickly dissected and placed into room temperature oxygenated (95% O_2-5% CO_2) NMDG-based solution. Frontal lobe area and cerebellum were removed from the brain. Left hemisphere of the brain was mounted on the stage of a Vibrating Microtome 7000 (Campden Instruments LTD, England, UK) and the first 3-4 hippocampal slices (400 µm) from the dorsal part of the hemisphere were cut at horizontal plane. During recovery period freshly prepared slices were incubated at 34°C for 12 min in oxygenated NMDG solution. After that slices were transferred to submerged type storage chamber and maintained at a room temperature for at least 2 h before use in an oxygenated artificial cerebrospinal fluid (ACSF) of the following composition (mM): 119 NaCl, 3 KCl, 2.0 $CaCl_2$, 1.3 $MgSO_4$, 1.2 NaH_2PO_4, 26 $NaHCO_3$ and 11 glucose, pH 7.35.

Slices were transferred to the interface type recording chamber and perfused with oxygenated ACSF (1.5-2 mL/min). The temperature in the chamber was maintained at

25-26°C (PTC03, Scientific Systems Design, Ontario, Canada). Extracellular field excitatory postsynaptic potential (fEPSP) recordings were obtained from the hippocampal CA1 stratum radiatum using Differential AC Amplifier 1700 (A-M Systems, Carlsborg, WA, USA). The recording electrode was an Ag/AgCl wire in ACSF-filled extracellular glass microelectrode (1-1.5 MΩ). Evoked postsynaptic responses were elicited by stimulation of Schaffer collaterals using a bipolar stimulating electrode and DS3 Isolated current stimulator (Digitimer Ltd, Hertfordshire, UK). Synaptic response profiles were determined by generating input–output curve (stimulation intensity between 10 and 100 μA, 100 μs) for each slice. No significant differences were found in the input-output curve between genotypes. The input-output profile of the slice was used to set the stimulation strength for long term potentiation (LTP) experiments. For LTP experiments, the stimulation intensity was set to elicit 30% of maximal fEPSP slope. This resulted in different absolute stimulus intensity between slices and animals; however, this paradigm ensured that the recruitment of synapses was standardised relative to the overall excitability of the slice. Data were normalized to pre-tetanus for all groups which also controls for stimulus intensity differences. For pre- and post-tetanus stimulation, the stimulation was applied every 30 s. After 10-20 min of stable baseline recording high-frequency tetanic stimulation (HFS, 100 Hz, 1 s) was delivered. Data was amplified x100, band-pass filtered (1Hz – 5kHz) and digitized at 20.8 or 20.06kHz using an analogue-to-digital converter (National Instruments, Austin, TX) and acquired using WinWCP (Strathclyde Electrophysiology Software, Glasgow, UK).

Offline data analysis was performed using ClampFit (Axon Instruments, USA). The fEPSP slope was calculated between 2 manually positioned cursors. The first cursor was positioned at the rising inflection of the fEPSP after the fiber volley. The second cursor was set to measure the slope of monosynaptic EPSP, and placed before the point where the rising slope began levelling off, to exclude population spikes.

Immunohistochemistry

For immunohistochemical analysis, mice were sacrificed by terminal anesthesia at 9 months of age after completing behavioural tests. The animals were perfused with phosphate buffer saline, brains were dissected, and one hemisphere fixed for 48 hours in 4% paraformaldehyde with 15% glycerol cryoprotectant. The other hemisphere had tissue from entorhinal cortex and hippocampus prepared for array tomography as described previously (Kay *et al.*, 2013; Pickett *et al.*, 2019). Coronal sections, 50 μm in thickness, were cut through the entire fixed hemisphere. Every 20th section from n=5 mice per group was stained with pan Aβ antibody AW7 (a generous gift from Prof Dominic Walsh) and plaque fibrils counterstained with 0.05% Thioflavin S in 50% ethanol. Images were acquired on a Zeiss AxioImager microscope with a 20x objective. For array tomography, embedded tissue blocks were sectioned with an ultracut microtome (Zeiss) into ribbons of 70nm serial sections. Ribbons were stained with primary antibodies at 1:50 dilution in blocking buffer AW7 (secondary - donkey anti rabbit 488, Invitrogen) one of the following tau antibodies: Total Tau (Gt, R&D

systems, secondary donkey anti goat 594, Invitrogen), PhF1 (a generous gift from Peter Davies, secondary donkey anti mouse 594, Invitrogen), Alz50 (from Peter Davies, secondary antibody donkey anti mouse IgM 594, Invitrogen), or CP13 (from Peter Davies, secondary antibody donkey anti mouse 594, Invitrogen). After secondary antibody staining, nuclei were counterstained with DAPI, coverslips were mounted with ImmuMount, and images acquired on a Ziess AxioImager microscope with a 63x, 1.4NA objective.

Data analysis

Statistical analyses were performed and graphs generated in R Studio v1.2.1335 running R package version 5.2.2. For novel object recognition discrimination ratios, each genotype was compared to the hypothetical discrimination ratio of d=0 using a one-sample t-test. P values were corrected for multiple comparisons with a Holm adjustment. Data were checked for normality with Shapiro-Wilks normality tests. To examine differences between genotypes and look for sex effects in the APP/PS1+Tau line behavioural studies at 9-10.5 months of age, linear mixed effects models were used with the experimental batch as a random variable with the formula: lmer(Variable_of_Interest~Genotype+Sex+(1|testing_batch)). To examine effects of age on behavioural phenotypes in APP/PS1+Tau and control genotypes, a linear mixed effects model was used which accounted for 2 batches of testing and multiple measurements per animal as follows: lmer(Variable_of_Interest~Genotype*Age+Sex+(1|testing_batch)+(1|Mouse_ID)).

Assumptions of the models were tested using visual inspection of the Q-Q plot of residuals. To test correlations between variables, Spearman's rank correlations were performed followed by Holm adjustments for multiple comparisons.

For LTP data, the average fEPSP slope during a 10 min period before LTP induction was taken as the baseline, and values were normalized to this value. Potentiation was measured between 50 to 60 min after HFS. To avoid pseudoreplication, a mean normalised fEPSP slope was calculated across slices per animal. This mean normalised fEPSP slope was used in statistical comparison between groups and in plotting the time course of LTP. Statistical analysis was carried out using R. Normality of fEPSP slope data was tested using a Shapiro-Wilk normality test. Two groups did not meet normality due to low sample size (APP/PS1+Tau, n=5) and the presence of a single outlier (Tau). For these groups, results from both parametric and non-parametric tests are reported for LTP testing. For between group comparisons, homogeneity of variances was tested using the Bartlett test ($p>0.05$).

Results are reported as box and whisker plots showing each measured value as an individual data point alongside the median (centre line) 75th percentile (top of box) 25th percentile (bottom of box), largest value within 1.5 times interquartile range above 75th percentile (top whisker), smallest value within 1.5 times interquartile range below 25th percentile (bottom whisker). LTP data and line graphs show mean ± SEM, Scatter plots show individual data points and linear regression lines with 95% confidence intervals.

Data accessibility

Data used in this manuscript are provided in supplemental tables associated with the paper. For detailed raw files (e.g. movies of mice doing novel object recognition), contact authors.

Results:

To test the hypothesis that memory was impaired in APP/PS1+Tau mice, novel object recognition memory was assessed in mice between 9 and 10.5 months of age, a time point when we previously observed a hyperactivity behavioural phenotype alongside transcriptional dysregulation (Pickett *et al.*, 2019). Fig1a shows that as previously reported, these APP/PS1+Tau mice move farther in the open field, a behavioural measure of hyperactivity (linear mixed effects model APP/PS1+Tau vs control $p<0.001$, full statistics in supplemental table 5). Mice are innately curious and prefer to explore novel over familiar objects. A discrimination ratio in novel object recognition testing above 0 indicates preference for the novel object reflecting memory of which object was previously explored. Novel object memory testing did not uphold our hypothesis as all 4 genotypes exhibited significant novel object recognition memory at this age (Figure 1b). For all groups, the discrimination ratio was significantly different from 0 as determined by one-sample t-tests. After Holm correction for multiple testing, the p values for each group were below 0.001 (please see supplemental table 6 for exact t-statistics and p-values). We used a linear mixed

effects model to determine whether there were differences between genotypes or any sex effects while taking into account the testing was run in 2 batches (with testing batch as a random variable in the model). This model indicates there were no differences between genotypes in novel object recognition nor were there any differences between male and female mice (supplemental table 7 contains the results of the model). The total amount of time mice explored the objects (exploration time) was examined as differing exploration times could contribute to differences in memory. Although all groups exhibited novel object recognition memory, there were significant differences between groups and between sexes in exploration time (Figure 1c). A linear mixed effects model reveals that tau mice and APP/PS1+Tau mice explore significantly more than control mice and females explore more than males (supplemental table 8). However, in our dataset, we do not see a correlation in any group between exploration time and novel object discrimination ratio (Figure 1d, Spearman correlation p values >0.3 for all genotypes). Thus, in our mice, the different exploration times between groups is unlikely to affect novel object memory (for similar results see Akkerman *et al.*, 2012). Many previous studies have reported novel object recognition deficits in APP/PS1 at ages when plaque deposition was evident (Pedrós *et al.*, 2014; Gu *et al.*, 2016; Shen *et al.*, 2017). We previously reported plaque deposition in these APP/PS1+Tau mice starting by 6 months of age (Pickett *et al.*, 2019). Further, we previously reported that Aβ levels in the brain are approximately 15 pg/mg total protein and are not different between APP/PS1 and APP/PS1+Tau mice and tau protein levels are approximately 10 ng/mg total protein

and do not differ between APP/PS1+Tau mice and Tau mice (Pickett *et al.*, 2019). Since both plaques and tangles have been associated in mice with spatial memory disruption, we stained for plaques and phosphorylated tau. We confirm in this study that both APP/PS1+Tau mice and littermate APP/PS1 mice at 9 months of age have substantial plaque deposition (Figure 1e,f). In the APP/PS1+Tau mice, there are small accumulations of phosphorylated tau around plaques, but no neurofibrillary tangle pathology as we previously reported (Figure 1f). High resolution array tomography imaging shows accumulation of small punctae of tau staining in multiple forms (1g), total tau, phosphoTau labelled with PHF1 and CP13 antibodies, and misfolded tau labelled with Alz50 antibody. To determine whether the lack of novel object recognition in 9-10.5 month old APP/PS1+Tau mice was due to a delay in the phenotype compared to the parent APP/PS1 line with endogenous mouse tau, we completed an ageing study in these mice testing memory out to 14 months of age (Figure 1g,h). Two cohorts of mice were tested, one at 3, 6, and 9 months of age, and another at 10.5 and 14 months of age. APP/PS1+Tau mice still have intact novel object recognition memory at 14 months of age (one-sided t-test adjusted p value = 0.023), and a linear mixed effects model reveals there is not a significant effect of genotype, age, or sex on memory (supplemental table 9). There are age and sex effects on exploration time, but no genotype effects (supplemental table 10). Rotarod testing was used to determine if there were motor deficits in this line. Subtle changes in latency to fall off the rotarod were observed between sexes and in tau mice compared to controls (Supplemental figure 1, supplemental table 11), however

these were likely to be driven by the CKtTA activator transgene as will be discussed later.

To determine whether the lack of memory phenotype in these mice was due to lack of endogenous mouse tau and to confirm that in our hands the novel object recognition test can detect memory deficits in an established model, we tested the parent APP/PS1 line from Jackson labs that have endogenous mouse tau. As expected, APP/PS1 mice with endogenous mouse tau had novel object recognition deficits at 9 months of age, with their discrimination ratios being not significantly different from zero (one-sample t-test adjusted p-value=0.489) whereas wild-type littermates had a significant preference for the novel object (one-sample t-test adjusted p-value=0.008, Figure 2a). This memory deficit was not due to differences in total time exploring the objects which were not different between the 2 groups (Figure 2b). As observed in the APP/PS1+Tau line and littermate controls, there was also no correlation between novel object recognition and exploration time in APP/PS1 mice with endogenous mouse tau or their wild-type littermates (Spearman rank correlation adjusted p-value=1.000 for both groups, Figure 2c).

As a further control, we examined novel object recognition memory in mice expressing only the CKtTA transactivator gene. This is important as this transgene is used in APP/PS1+Tau mice to drive human tau expression, and we previously observed this transgene affects brain weight in mice (Pickett *et al.*, 2019). Here we observe that there was no effect of this transgene on novel object recognition. Both

CKtTA and littermate control mice have intact recognition memory (one-sample t-tests adjusted p-value<0.05 for both groups Figure 2d) and there is no difference between genotypes or sexes (linear mixed effects model with testing batch as a random variable, Supplemental table 12). Compared to controls, there is no effect of this transgene or sex on exploration time in the CKtTA mice (linear mixed effects model with testing batch as a random variable, Supplemental Table 13, Figure 2e). There was also no correlation between novel object recognition discrimination ratio and exploration time (Spearman rank correlation adjusted p-value=1.000 for both groups, Figure 2f). There was a significant rotarod deficit in CKtTA mice (supplemental figure 1, supplemental table 14), indicating that the driver transgene in the absence of tau expression is sufficient to cause a motor phenotype. However, this did not cause an impairment of the ability to explore objects nor did it cause memory deficits.

To assay hippocampal LTP, we tetanized the Schaffer collateral pathway. Intact LTP was observed in control, APP/PS1, and Tau genotypes at 9-10.5 months of age (Figure 3; Wilcoxon test baseline = 100% - control: 138%, IQR 41%, V=91, adjusted p=0.001; APP/PS1: 126%, IQR 12%, V=66, p=0.039; Tau: 137%, IQR 21%, V=45, p=0.016). In APP/PS1+Tau mice at this age, although the EPSP slope 60 minutes after tetanisation was 122% of baseline, this did not reach significance (IQR 10%, V=15, p=0.06, adjusted p=0.25). However, we are hesitant to interpret this as a loss of LTP since there is no significant difference in the extent of potentiation between

genotypes in the APP/PS1+Tau cohort (Kruskall-Wallis $Chi^2(3)=1.72$, p=0.63), and the lack of significance in the APP/PS1+Tau group may be driven by the smaller group size, a limitation of the number of animals available for experiments in this complex cross.

In WT mice with endogenous mouse tau, tetanization resulted in a significant potentiation of the fEPSP slope measured in CA1 stratum radiatum (129 ± 8.7% of baseline, t(5)=3.4, Holm adjusted p=0.04, 2-tailed, one-sample t-test compared to mean of 100%). In APP/PS1 littermates with endogenous mouse tau, the same stimulation paradigm did not induce significant potentiation (109.9 ± 7.1% of baseline, t(6)= 1.4, Holm adjusted p= 0.43 2-tailed, one-sample t-test compared to mean of 100%; Figure 3). Together, these data indicate that tau is needed to drive LTP deficits in APP/PS1 mice.

Discussion:

Understanding the cascade from early Aβ accumulation through pathological tau accumulation to neural circuit dysfunction and neurodegeneration remains one of the key challenges facing the Alzheimer's disease field (Karran *et al.*, 2011; Mauricio *et al.*, 2019), and there are relatively few studies directly addressing the cooperation of Aβ and tau in disrupting memory and synaptic plasticity.

Our previous work in the APP/PS1+Tau mouse line and human postmortem tissue indicate that both Aβ and tau accumulate in synapses, where it may contribute to synaptic dysfunction and downstream cognitive decline (Jackson *et al.*, 2016, 2019; Zhou *et al.*, 2017; McInnes *et al.*, 2018; Hesse *et al.*, 2019; Pickett *et al.*, 2019). Similar to findings by Chabrier *et al.*, 2012, who expressed mutant APP and wild-type human tau, in the APP/PS1+Tau line, we observe tau accumulation in post synapses, which is associated with a behavioural hyperactivity phenotype (Pickett *et al.*, 2019). In contrast, we did not observe memory deficits in APP/PS1+Tau mice . This discrepancy could reflect that the mice in Chabrier et al retained endogenous mouse tau in addition to expressing wild-type human tau, and mouse tau is known to be important for synaptic phenotypes induced by Aβ (Roberson *et al.*, 2011; Shipton *et al.*, 2011).

Indeed, we confirm the importance of mouse tau driving Aβ phenotypes in this study as we observe that APP/PS1 mice expressing endogenous mouse tau do exhibit both novel object memory and LTP deficits at 9-10.5 months of age as has been reported previously (Pedrós *et al.*, 2014; Gu *et al.*, 2016; Shen *et al.*, 2017)(Cai *et al.*, 2017; Wu *et al.*, 2017). Whereas in agreement with previous reports indicating that lowering endogenous mouse tau protects APP overexpressing mice (Ittner *et al.*, 2010; Vossel *et al.*, 2010; Roberson *et al.*, 2011; Shipton *et al.*, 2011; DeVos *et al.*, 2018), here we observe that APP/PS1 mice on a MAPTnull background do not have novel object recognition or LTP deficits compared to littermate controls.

Surprisingly, expression of human tau in these mice did not simply reconstitute the behaviour and plasticity deficits seen in APP/PS1 mice with mouse tau. These data indicate that the differences between mouse and human tau may be important in mediating the synaptotoxic effects of Aβ. Alternatively, the overexpression of human tau in our APP/PS1+Tau line with the CamKII promotor controlled CKtTA transactivator does not result in normal spatiotemporal expression of tau and has higher levels than endogenous mouse tau, which may affect the interactions with Aβ. Either way, our results support the need for the use of multiple models alongside descriptive human tissue studies to ensure translational relevance of mouse studies in the Alzheimer's field.

Author contributions:

Designed study (I.O., O.H., T.L.S.-J.), conducted experiments (J.T., O.N., E.K.P., A.G.H., P.J.), analysed data (O.N., E.K.P., A.G.H., A.S., I.O., T.L.S.-J.), drafted paper (T.L.S.-J.).

Acknowledgements:

This work was funded by the European Research Council (ERC) under the European Union's Horizon 2020 research and innovation programme (Grant agreement No. 681181), the UK Dementia Research Institute which receives its funding from DRI Ltd, funded by the UK Medical Research Council, Alzheimer's Society, and Alzheimer's Research UK, Alzheimer's Research UK and the Scottish Government Chief Scientist Office (ARUK SPG2013-1), a Wellcome Trust Translational Neuroscience PhD studentship, and Alzheimer's Society.

Competing interests: TS-J is on the Scientific Advisory Board of Cognition Therapeutics and receives collaborative grant funding from 2 industry partners. None of these had any influence over the current paper.

References:

Akkerman, S., Blokland, A., Reneerkens, O., van Goethem, N.P., Bollen, E., Gijselaers, H.J.M., Lieben, C.K.J., Steinbusch, H.W.M., & Prickaerts, J. (2012) Object recognition testing: methodological considerations on exploration and discrimination measures. *Behav. Brain Res.*, **232**, 335–347.

Cai, H., Wang, Y., He, J., Cai, T., Wu, J., Fang, J., Zhang, R., Guo, Z., Guan, L., Zhan, Q., Lin, L., Xiao, Y., Pan, H., & Wang, Q. (2017) Neuroprotective effects of bajijiasu against cognitive impairment induced by amyloid-β in APP/PS1 mice. *Oncotarget*, **8**, 92621–92634.

Chabrier, M.A., Blurton-Jones, M., Agazaryan, A.A., Nerhus, J.L., Martinez-Coria, H., & LaFerla, F.M. (2012) Soluble Aβ Promotes Wild-Type Tau Pathology In Vivo. *J. Neurosci.*, **32**, 17345–17350.

DaRocha-Souto, B., Scotton, T.C., Coma, M., Serrano-Pozo, A., Hashimoto, T., Serenó, L., Rodríguez, M., Sánchez, B., Hyman, B.T., & Gómez-Isla, T. (2011) Brain Oligomeric β-Amyloid but Not Total Amyloid Plaque Burden Correlates With Neuronal Loss and Astrocyte Inflammatory Response in Amyloid Precursor Protein/Tau Transgenic Mice. *J Neuropathol Exp Neurol*, **70**, 360–376.

DeVos, S.L., Corjuc, B.T., Commins, C., Dujardin, S., Bannon, R.N., Corjuc, D., Moore, B.D., Bennett, R.E., Jorfi, M., Gonzales, J.A., Dooley, P.M., Roe, A.D., Pitstick, R., Irimia, D., Frosch, M.P., Carlson, G.A., & Hyman, B.T. (2018) Tau reduction in the presence of amyloid-β prevents tau pathology and neuronal death in vivo. *Brain*, **141**, 2194–2212.

Gu, X.-H., Xu, L.-J., Liu, Z.-Q., Wei, B., Yang, Y.-J., Xu, G.-G., Yin, X.-P., & Wang, W. (2016) The flavonoid baicalein rescues synaptic plasticity and memory

deficits in a mouse model of Alzheimer's disease. *Behavioural Brain Research*, **311**, 309–321.

Hardy, J.A. & Higgins, G.A. (1992) Alzheimer's disease: the amyloid cascade hypothesis. *Science*, **256**, 184-.

Henstridge, C.M., Hyman, B.T., & Spires-Jones, T.L. (2019) Beyond the neuron-cellular interactions early in Alzheimer disease pathogenesis. *Nat. Rev. Neurosci.*, **20**, 94–108.

Hesse, R., Hurtado, M.L., Jackson, R.J., Eaton, S.L., Herrmann, A.G., Colom-Cadena, M., Tzioras, M., King, D., Rose, J., Tulloch, J., McKenzie, C.-A., Smith, C., Henstridge, C.M., Lamont, D., Wishart, T.M., & Spires-Jones, T.L. (2019) Comparative profiling of the synaptic proteome from Alzheimer's disease patients with focus on the APOE genotype. *Acta Neuropathologica Communications*, **7**, 214.

Hoover, B.R., Reed, M.N., Su, J., Penrod, R.D., Kotilinek, L.A., Grant, M.K., Pitstick, R., Carlson, G.A., Lanier, L.M., Yuan, L.-L., Ashe, K.H., & Liao, D. (2010) Tau Mislocalization to Dendritic Spines Mediates Synaptic Dysfunction Independently of Neurodegeneration. *Neuron*, **68**, 1067–1081.

Ittner, L.M., Ke, Y.D., Delerue, F., Bi, M., Gladbach, A., van Eersel, J., Wölfing, H., Chieng, B.C., Christie, M.J., Napier, I.A., Eckert, A., Staufenbiel, M., Hardeman, E., & Götz, J. (2010) Dendritic function of tau mediates amyloid-beta toxicity in Alzheimer's disease mouse models. *Cell*, **142**, 387–397.

Jackson, R.J., Rose, J., Tulloch, J., Henstridge, C., Smith, C., & Spires-Jones, T.L. (2019) Clusterin accumulates in synapses in Alzheimer's disease and is increased in apolipoprotein E4 carriers. *Brain Commun*, **1**, fcz003.

Jackson, R.J., Rudinskiy, N., Herrmann, A.G., Croft, S., Kim, J.M., Petrova, V., Ramos-Rodriguez, J.J., Pitstick, R., Wegmann, S., Garcia-Alloza, M., Carlson, G.A., Hyman, B.T., & Spires-Jones, T.L. (2016) Human tau increases amyloid β plaque size but not amyloid β-mediated synapse loss in a novel mouse model of Alzheimer's disease. *Eur J Neurosci*, **44**, 3056–3066.

Jankowsky, J.L., Fadale, D.J., Anderson, J., Xu, G.M., Gonzales, V., Jenkins, N.A., Copeland, N.G., Lee, M.K., Younkin, L.H., Wagner, S.L., Younkin, S.G., & Borchelt, D.R. (2004) Mutant presenilins specifically elevate the levels of the

42 residue beta-amyloid peptide in vivo: evidence for augmentation of a 42-specific gamma secretase. *Hum. Mol. Genet.*, **13**, 159–170.

Karran, E., Mercken, M., & Strooper, B.D. (2011) The amyloid cascade hypothesis for Alzheimer's disease: an appraisal for the development of therapeutics. *Nature Reviews Drug Discovery*, **10**, 698–712.

Kay, K.R., Smith, C., Wright, A.K., Serrano-Pozo, A., Pooler, A.M., Koffie, R., Bastin, M.E., Bak, T.H., Abrahams, S., Kopeikina, K.J., McGuone, D., Frosch, M.P., Gillingwater, T.H., Hyman, B.T., & Spires-Jones, T.L. (2013) Studying synapses in human brain with array tomography and electron microscopy. *Nature Protocols*, **8**, 1366–1380.

Klein, W.L. (2013) Synaptotoxic Amyloid-β Oligomers: A Molecular Basis for the Cause, Diagnosis, and Treatment of Alzheimer's Disease? *Journal of Alzheimer's Disease*, **33**, S49–S65.

Koffie, R.M., Hyman, B.T., & Spires-Jones, T.L. (2011) Alzheimer's disease: synapses gone cold. *Mol Neurodegener*, **6**, 63.

Koffie, R.M., Meyer-Luehmann, M., Hashimoto, T., Adams, K.W., Mielke, M.L., Garcia-Alloza, M., Micheva, K.D., Smith, S.J., Kim, M.L., Lee, V.M., Hyman, B.T., & Spires-Jones, T.L. (2009) Oligomeric amyloid beta associates with postsynaptic densities and correlates with excitatory synapse loss near senile plaques. *Proc Natl Acad Sci U S A*, **106**, 4012–4017.

Li, S., Hong, S., Shepardson, N.E., Walsh, D.M., Shankar, G.M., & Selkoe, D. (2009) Soluble Oligomers of Amyloid β Protein Facilitate Hippocampal Long-Term Depression by Disrupting Neuronal Glutamate Uptake. *Neuron*, **62**, 788–801.

Masuda, A., Kobayashi, Y., Kogo, N., Saito, T., Saido, T.C., & Itohara, S. (2016) Cognitive deficits in single App knock-in mouse models. *Neurobiology of Learning and Memory*, MCCS 2016, **135**, 73–82.

Mauricio, R., Benn, C., Davis, J., Dawson, G., Dawson, L.A., Evans, A., Fox, N., Gallacher, J., Hutton, M., Isaac, J., Jones, D.N.C., Jones, L., Lalli, G., Libri, V., Lovestone, S., Moody, C., Noble, W., Perry, H., Pickett, J., Reynolds, D., Ritchie, C., Rohrer, J.D., Routledge, C., Rowe, J., Snyder, H., Spires-Jones, T., Swartz, J., Truyen, L., Whiting, P., & Therapeutics for Dementia Consortium (2019) Tackling gaps in developing life-changing treatments for dementia. *Alzheimers Dement (N Y)*, **5**, 241–253.

McInnes, J., Wierda, K., Snellinx, A., Bounti, L., Wang, Y.-C., Stancu, I.-C., Apóstolo, N., Gevaert, K., Dewachter, I., Spires-Jones, T.L., Strooper, B.D., Wit, J.D., Zhou, L., & Verstreken, P. (2018) Synaptogyrin-3 Mediates Presynaptic Dysfunction Induced by Tau. *Neuron*, **97**, 823-835.e8.

Oddo, S., Caccamo, A., Shepherd, J.D., Murphy, M.P., Golde, T.E., Kayed, R., Metherate, R., Mattson, M.P., Akbari, Y., & LaFerla, F.M. (2003) Triple-transgenic model of Alzheimer's disease with plaques and tangles: intracellular Abeta and synaptic dysfunction. *Neuron*, **39**, 409–421.

Pedrós, I., Petrov, D., Allgaier, M., Sureda, F., Barroso, E., Beas-Zarate, C., Auladell, C., Pallàs, M., Vázquez-Carrera, M., Casadesús, G., Folch, J., & Camins, A. (2014) Early alterations in energy metabolism in the hippocampus of APPswe/PS1dE9 mouse model of Alzheimer's disease. *Biochimica et Biophysica Acta (BBA) - Molecular Basis of Disease*, **1842**, 1556–1566.

Pickett, E.K., Herrmann, A.G., McQueen, J., Abt, K., Dando, O., Tulloch, J., Jain, P., Dunnett, S., Sohrabi, S., Fjeldstad, M.P., Calkin, W., Murison, L., Jackson, R.J., Tzioras, M., Stevenson, A., d'Orange, M., Hooley, M., Davies, C., Colom-Cadena, M., Anton-Fernandez, A., King, D., Oren, I., Rose, J., McKenzie, C.-A., Allison, E., Smith, C., Hardt, O., Henstridge, C.M., Hardingham, G.E., & Spires-Jones, T.L. (2019) Amyloid Beta and Tau Cooperate to Cause Reversible Behavioral and Transcriptional Deficits in a Model of Alzheimer's Disease. *Cell Reports*, **29**, 3592-3604.e5.

Roberson, E.D., Halabisky, B., Yoo, J.W., Yao, J., Chin, J., Yan, F., Wu, T., Hamto, P., Devidze, N., Yu, G.-Q., Palop, J.J., Noebels, J.L., & Mucke, L. (2011) Amyloid-β/Fyn-induced synaptic, network, and cognitive impairments depend on tau levels in multiple mouse models of Alzheimer's disease. *J. Neurosci.*, **31**, 700–711.

Roberson, E.D., Scearce-Levie, K., Palop, J.J., Yan, F., Cheng, I.H., Wu, T., Gerstein, H., Yu, G.-Q., & Mucke, L. (2007) Reducing Endogenous Tau Ameliorates Amyloid ß-Induced Deficits in an Alzheimer's Disease Mouse Model. *Science*, **316**, 750–754.

Sasaguri, H., Nilsson, P., Hashimoto, S., Nagata, K., Saito, T., De Strooper, B., Hardy, J., Vassar, R., Winblad, B., & Saido, T.C. (2017) APP mouse models for Alzheimer's disease preclinical studies. *EMBO J*, **36**, 2473–2487.

Shen, L., Han, B., Geng, Y., Wang, J., Wang, Z., & Wang, M. (2017) Amelioration of cognitive impairments in APPswe/PS1dE9 mice is associated with metabolites alteration induced by total salvianolic acid. *PLoS One*, **12**.

Shipton, O.A., Leitz, J.R., Dworzak, J., Acton, C.E.J., Tunbridge, E.M., Denk, F., Dawson, H.N., Vitek, M.P., Wade-Martins, R., Paulsen, O., & Vargas-Caballero, M. (2011) Tau Protein Is Required for Amyloid β-Induced Impairment of Hippocampal Long-Term Potentiation. *J. Neurosci.*, **31**, 1688–1692.

Spires-Jones, T.L. & Hyman, B.T. (2014) The intersection of amyloid beta and tau at synapses in Alzheimer's disease. *Neuron*, **82**, 756–771.

Tucker, K.L., Meyer, M., & Barde, Y.-A. (2001) Neurotrophins are required for nerve growth during development. *Nat Neurosci*, **4**, 29–37.

Vossel, K.A., Zhang, K., Brodbeck, J., Daub, A.C., Sharma, P., Finkbeiner, S., Cui, B., & Mucke, L. (2010) Tau reduction prevents Abeta-induced defects in axonal transport. *Science*, **330**, 198.

Wu, M., Shi, H., He, Y., Yuan, L., Qu, X., Zhang, J., Wang, Z., Cai, H., & Qi, J. (2017) Colivelin Ameliorates Impairments in Cognitive Behaviors and Synaptic Plasticity in APP/PS1 Transgenic Mice. *J. Alzheimers Dis.*, **59**, 1067–1078.

Yasuda, M. & Mayford, M.R. (2006) CaMKII Activation in the Entorhinal Cortex Disrupts Previously Encoded Spatial Memory. *Neuron*, **50**, 309–318.

Zhou, L., McInnes, J., Wierda, K., Holt, M., Herrmann, A.G., Jackson, R.J., Wang, Y.-C., Swerts, J., Beyens, J., Miskiewicz, K., Vilain, S., Dewachter, I., Moechars, D., De Strooper, B., Spires-Jones, T.L., De Wit, J., & Verstreken, P. (2017) Tau association with synaptic vesicles causes presynaptic dysfunction. *Nature Communications*, **8**, 1–13.

Figure 1: APP/PS1+Tau mice have intact object recognition memory despite plaque deposition. As previously reported (Pickett et al 2019), at 9-10.5 months of age, APP/PS1+Tau mice have a behavioural hyperactivity phenotype as they travel significantly farther than controls in the open field (a, * linear mixed effects model APP/PS1+Tau vs control $p<0.0001$). At this same age, all four genotypes in the APP/PS1+Tau cross have discrimination ratios significantly different from zero

indicating intact object memory (b, * one-sample t-test p<0.001). Exploration time differed between groups (c, * linear mixed effects model Tau vs control p=0.019). Performance in the novel object recognition test was unlikely affected by differences in exploration times as none of the groups exhibited a correlation between these measures (d, Spearman correlation each group p>0.3, linear regression lines shown alongside grey 95% confidence intervals). Staining with pan Aβ antibody AW7 (magenta), thioflavin S to label fibrils (cyan) and PHF1 phospho-tau antibody (yellow) shows plaques in hippocampus of both APP/PS1 and APP/PS1+Tau mice (e,f) and small accumulations of phospho-tau around plaques in APP/PS1+Tau mice (arrows, f). Higher resolution imaging with array tomography (g) reveals small accumulations of several forms of tau in APP/PS1+Tau mice: total tau, PHF1 positive tau phosphorylated at Ser396/404, CP13 positive tau phosphorylated at Ser202,and Alz50 positive misfolded tau. Examining averages of discrimination ratios per group over time (h) reveals that APP/PS1+Tau mice have intact object recognition memory up to 14 months of age (dotted line represents 2 different cohorts were tested at 3, 6, 9 months and 10.5, 14 months). Trajectories of individual mice are shown in (i). Individual mouse values are shown as points a-d with male mice indicated with circles and female mice with triangles. Numbers of mice per group are indicated over the boxes in box and whisker plots. Scale bar represents 100 microns in e,f, 10 microns in g.

Figure 2: APP/PS1 mice with endogenous mouse tau have deficits detecting in object memory assessed in a novel object recognition task at 9-10.5 months of age (a, one sided t-test null hypothesis zero, t-statistic=1.319, adjusted p-value=0.489), while their wild-type (wt) littermates express intact object memory as shown by a discrimination ratio significantly larger than zero (a, * one-sample t-test, t=5.003, adjusted p=0.0082). Exploration time was not different between wt and APP/PS1 mice and there was no effect of sex (b, two-way ANOVA effect of genotype F[1,8]=1.876, p=0.208, effect of sex F[1,8]=0.426, p=0.532). Scatterplots with linear regression lines and 95% confidence intervals (shaded in grey) show no correlation between discrimination ratio and exploration time in either genotype (c). The CKtTA driver transgene does not affect novel object recognition performance (d, * control

one-sample t-test, t =3.504, adjusted p =0.019; CKtTA t=3.230, adjusted p =0.0289) or exploration time (e) and there is no correlation between these variables. Points represent individual mice. Male mice are indicated with circles and female mice with triangles. n per group is shown above each box.

Figure 3: LTP was induced with tetanization at time 0 (arrows). In slices from the APP/PS1+Tau line cohort which lack endogenous mouse tau, all genotypes exhibit fEPSP slopes above baseline (a). At 50-60 minutes post-tetanization (b), control, APP/PS1, and tau mice exhibit significant potentiation but the APP/PS1+Tau group is not significantly different from baseline (* p<0.05 Wilcoxon test compared to 1.0 with Holm corrected p values). No significant differences were found in the input-output curve between genotypes (c). Representative traces for the APP/PS1+Tau cohort are shown in (d). In APP/PS1 mice with endogenous mouse tau, LTP was impaired at 9-10 months of age, while wild-type littermates exhibited significant LTP (e, f, * Holm adjusted p=0.04, one-sample t-test compared to mean of 1.0). Again, no significant differences were found in the input-output curve between genotypes (g). Representative traces for the APP/PS1 cohort are shown in (h). Data shown in a and e are means +/- standard error. Scale bars represent 10ms, 0.5mV. Points in box plots represent individual mice, n per group is shown above each box.

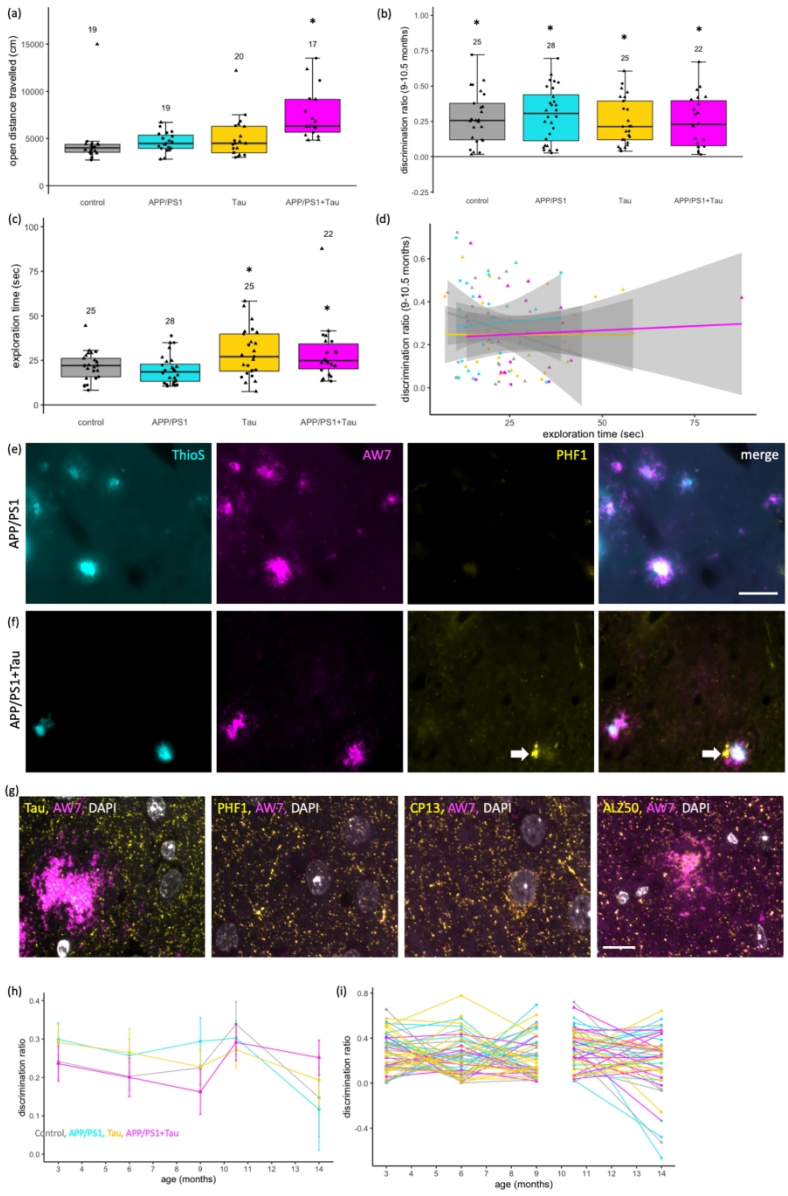

Figure 1: APP/PS1+Tau mice have intact object recognition memory despite plaque deposition. As previously reported (Pickett et al 2019), at 9-10.5 months of age, APP/PS1+Tau mice have a behavioural hyperactivity phenotype as they travel significantly farther than controls in the open field (a, * linear mixed effects model APP/PS1+Tau vs control $p<0.0001$). At this same age, all four genotypes in the APP/PS1+Tau cross have discrimination ratios significantly different from zero indicating intact object memory (b, * one-sample t-test $p<0.001$). Exploration time differed between groups (c, * linear mixed effects model Tau vs control $p=0.019$). Performance in the novel object recognition test was unlikely affected by differences in exploration times as none of the groups exhibited a correlation between these measures (d, Spearman correlation each group $p>0.3$, linear regression lines shown alongside grey 95% confidence intervals). Staining with pan A□ antibody AW7 (magenta), thioflavin S to label fibrils (cyan) and PHF1 phospho-tau antibody (yellow) shows plaques in hippocampus of both APP/PS1 and APP/PS1+Tau mice (e,f) and small accumulations of phospho-tau around plaques in APP/PS1+Tau mice (arrows, f). Higher resolution imaging with array tomography (g) reveals small accumulations of several forms of tau in APP/PS1+Tau mice: total tau, PHF1 positive tau phosphorylated at Ser396/404, CP13 positive tau phosphorylated at Ser202,and

Alz50 positive misfolded tau. Examining averages of discrimination ratios per group over time (h) reveals that APP/PS1+Tau mice have intact object recognition memory up to 14 months of age (dotted line represents 2 different cohorts were tested at 3, 6, 9 months and 10.5, 14 months). Trajectories of individual mice are shown in (i). Individual mouse values are shown as points a-d with male mice indicated with circles and female mice with triangles. Numbers of mice per group are indicated over the boxes in box and whisker plots. Scale bar represents 100 microns in e,f, 10 microns in g.

183x280mm (300 x 300 DPI)

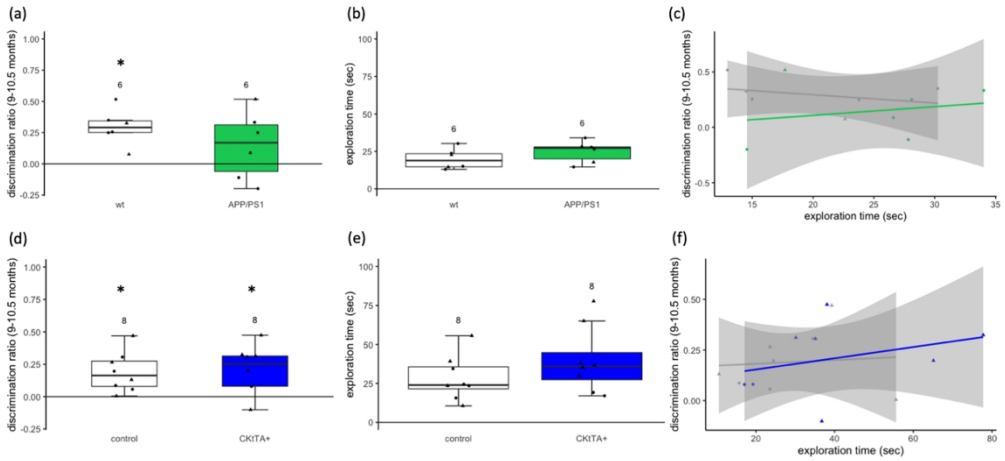

Figure 2: APP/PS1 mice with endogenous mouse tau have deficits detecting in object memory assessed in a novel object recognition task at 9-10.5 months of age (a, one sided t-test null hypothesis zero, t-statistic=1.319, adjusted p-value=0.489), while their wild-type (wt) littermates express intact object memory as shown by a discrimination ratio significantly larger than zero (a, * one-sample t-test, t =5.003, adjusted p =0.0082). Exploration time was not different between wt and APP/PS1 mice and there was no effect of sex (b, two-way ANOVA effect of genotype F[1,8]=1.876, p=0.208, effect of sex F[1,8]=0.426, p=0.532). Scatterplots with linear regression lines and 95% confidence intervals (shaded in grey) show no correlation between discrimination ratio and exploration time in either genotype (c). The CKtTA driver transgene does not affect novel object recognition performance (d, * control one-sample t-test, t =3.504, adjusted p =0.019; CKtTA t=3.230, adjusted p =0.0289) or exploration time (e) and there is no correlation between these variables. Points represent individual mice. Male mice are indicated with circles and female mice with triangles. n per group is shown above each box.

183x85mm (300 x 300 DPI)

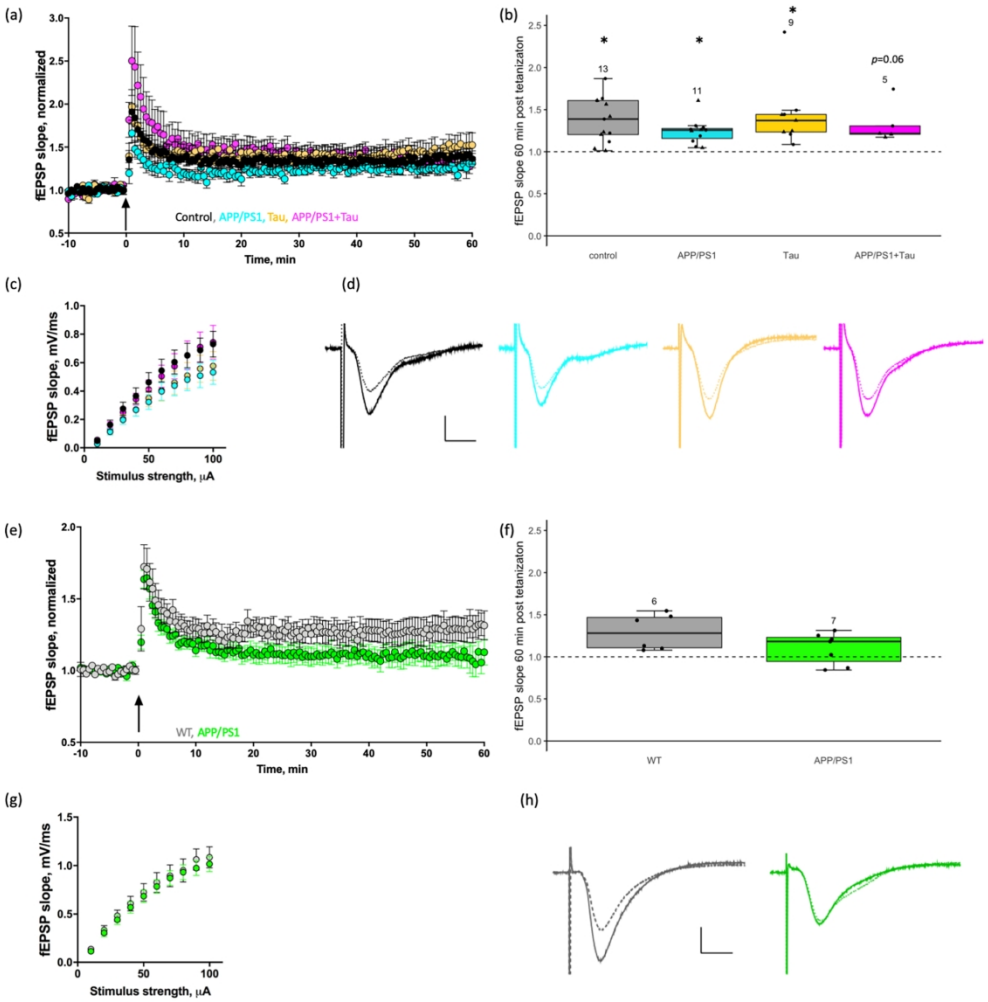

183x188mm (300 x 300 DPI)

Table 1: Summary of mice included in the study

APP/PS1+Tau cohort (total – all ages)					
	control (N=66)	**APP/PS1 (N=69)**	**Tau (N=66)**	**APP/PS1+Tau (N=50)**	**Overall (N=251)**
Sex					
m	30 (45.5%)	41 (59.4%)	31 (47.0%)	18 (36.0%)	120 (47.8%)
f	36 (54.5%)	28 (40.6%)	35 (53.0%)	32 (64.0%)	131 (52.2%)
APP/PS1+Tau 9-10.5 months of age behaviour cohort (subset of total above)					
	control (N=25)	**APP/PS1 (N=28)**	**Tau (N=25)**	**APP/PS1+Tau (N=22)**	**Overall (N=100)**
Sex					
m	10 (40.0%)	17 (60.7%)	11 (44.0%)	8 (36.4%)	46 (46.0%)
f	15 (60.0%)	11 (39.3%)	14 (56.0%)	14 (63.6%)	54 (54.0%)
APP/PS1+Tau 9-10.5 mo LTP cohort (also used in behaviour included in above)					
	control (N=13)	**APP/PS1 (N=11)**	**Tau (N=9)**	**APP/PS1+Tau (N=5)**	**Overall (N=38)**
Sex					
m	6 (46.2%)	4 (36.4%)	5 (55.6%)	2 (40.0%)	17 (44.7%)
f	7 (53.8%)	7 (63.6%)	4 (44.4%)	3 (60.0%)	21 (55.3%)
APP/PS1 cohort (9-10.5 months of age)					
	wt (N=9)	**APP/PS1 (N=12)**	**Overall (N=21)**		
Sex					
m	5 (55.6%)	11 (91.7%)	16 (76.2%)		
f	4 (44.4%)	1 (8.3%)	5 (23.8%)		
CKtTA cohort (9-10.5 months of age)					
	control (N=9)	**CKtTA+ (N=9)**	**Overall (N=18)**		
Sex					
m	5 (55.6%)	3 (33.3%)	8 (44.4%)		
f	4 (44.4%)	6 (66.7%)	10 (55.6%)		

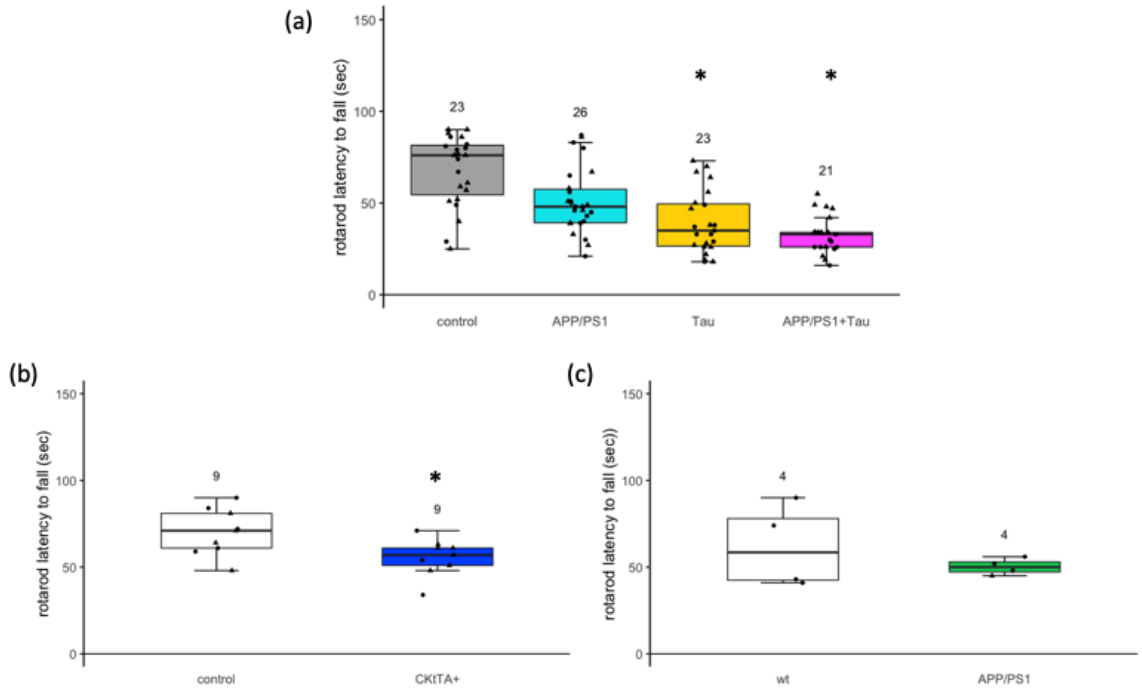

Supplemental figure 1: Rotarod testing indicates that the CKtTA driver transgene affects motor performance. In the APP/PS1+Tau line (a), there are significant differences in exploration time between Tau and control mice and APP/PS1+Tau and control mice (*, $p<0.05$ linear mixed effects model, supplemental table 11) and between male and female mice ($p=0.003$). This decrease in exploration time in the lines containing human tau is likely due not to tau expression but to the CKtTA activator transgene used to drive tau as in the parent CKtTA line (b), there is a significant decrease in CKtTA mice compared to controls (* $b=14.006$, $t=2.325$, $p=0.0345$) in the absence of human tau expression. In the APP/PS1 parent line with endogenous mouse tau, there is no difference between rotarod performance in APP/PS1 mice and wild-type littermates (c, one-way ANOVA $F[1,6]=0.921$, $p=0.374$), indicating that the observed memory deficits were not due to alterations in gross motor skills. Note mice that jumped off of the rotarod instead of running until they fell were excluded from this analysis. This precluded analysis of sex effects in the APP/PS1 line.

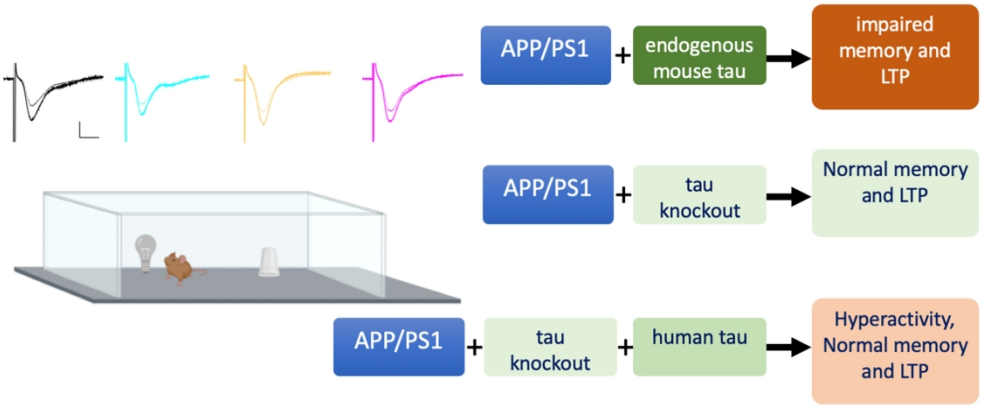

183x81mm (300 x 300 DPI)

Graphical Abstract Text

Tulloch *et al* observe memory and long-term potentiation deficits in the APP/PS1 mouse model of familial Alzheimer's disease, which are prevented by genetic removal of endogenous mouse tau. Expression of human tau in APP/PS1 mice with endogenous tau knockout does not reinstate the memory and plasticity deficits. These results highlight the importance of understanding differences between mouse and human tau in modelling Alzheimer's disease.